Purification and characterization of NADP-isocitrate dehydrogenase from skeletal muscle of Urocitellus richardsonii.

Isabelle A. MacLean
  University of Toronto
Anchal Varma
  Carleton University
Kenneth B Storey (✉ kenstorey@cunet.carleton.ca)
  Carleton University   https://orcid.org/0000-0002-2280-7599

Research Article

Abstract

NADP-dependent isocitrate dehydrogenase (NADP-IDH, EC 1.1.1.42) catalyzes the oxidative decarboxylation of isocitrate to α-ketoglutarate with the concomitant production of NADPH. NADPH plays important roles in many biosynthesis pathways, maintenance of proper oxidation-reduction balance, and protection against oxidative damage. This present study investigated the dynamic nature of NADP-IDH during hibernation by purifying it from the skeletal muscle of Richardson's ground squirrel (*Urocitellus richardsonii*) and analyzing its structural and functional changes in response to hibernation. Kinetic parameters of purified NADP-IDH from euthermic and hibernating ground squirrel skeletal muscle were characterized at 22°C and 5°C. Relative to euthermic muscle, NADP-IDH in hibernating muscle had a higher affinity for its substrate, isocitrate at 22°C, whereas at 5°C, there was a significant decrease in isocitrate affinity. Western blot analysis revealed greater serine and threonine phosphorylation in hibernator NADP-IDH as compared to euthermic NADP-IDH. In addition, Bioinformatic analysis predicted the presence of 18 threonine and 21 serine phosphorylation sites on squirrel NADP-IDH. The structural and functional changes in NADP-IDH indicate the ability of the organism to reduce energy consumption during hibernation, while emphasizing increased NADPH production, and thus antioxidant activity, during torpor arousal cycles.

1. Introduction

Hibernation is a well-known phenomenon which enables many mammals to withstand harsh winter conditions. During hibernation, they typically enter a hypometabolic state to reduce their metabolic expenditure in extreme conditions. This 'energy saving' state is characterized by suppression of metabolic rate and lowering of body temperature to conserve energy [1]. Richardson's ground squirrels (*Urocitellus richardsonii*) are obligate hibernators that possess the ability to drop their metabolic rate by approximately 95% relative to their euthermic state [2, 3]. Overall, this allows these mammals to conserve about 88% of their energy [2−4]. The most obvious vital changes during hibernation are the reduction of heart rate, breathing rate and body temperature, along with the biochemical adaptations that mediate the entry, maintenance, and exit from a hypometabolic state [4, 5]. During hibernation, there is a notable change in fuel source, with hibernating mammals switching from carbohydrates as a main source for energy to the oxidation of stored triglycerides in adipose tissue [6, 7]. The marked changes in metabolic demand during hibernation is strictly controlled and coordinated by the regulation of gene expression and enzyme function [8−10]. The major regulatory mechanism that mediates the entry into the hypometabolic state is reversible phosphorylation of enzymes and proteins [11, 12].

NADP-dependent isocitrate dehydrogenase (NADP-IDH, EC 1.1.1.42) is a highly regulated enzyme in the tricarboxylic acid cycle, which is a crucial pathway in energy metabolism and biosynthesis. It catalyzes the oxidative decarboxylation of isocitrate into alpha-ketoglutarate with the concomitant production of NADPH [13]. The enzyme is thus dependent on isocitrate, NADP, and an additional metal cofactor, Mg^{2+}, to carry out the alpha-ketoglutarate producing reaction. NADPH is known for acting as an important cofactor for various metabolic processes [14]. As contribution of NADP-IDH to NADPH production is

significant, it is possible that the regulation of NADP-IDH enzymatic activity may have an indirect effect on the metabolism of animals during hibernation. NADPH is often necessary in various antioxidant reactions making the regulation of its production critically important, as this can be a key for the survivability of ground squirrels and other organisms undergoing hibernation. This present study explores the regulation of NADP-IDH in hibernating *U. richardsonii* skeletal muscle. Assessments on the kinetic activity of the enzyme were explored in addition to determination of phosphorylation status in the euthermic versus hibernating state as a potential mechanism to facilitate any observed kinetic changes. Bioinformatic analysis of the enzyme was performed to observe the viability of phosphorylation sites, as well as to determine potential enzyme structure, sequence similarity, and size.

2. Materials And Methods

2.1 Animal treatments

Richardson's ground squirrels (*Urocitellus richardsonii*) were caught in the summer near Calgary, Alberta. They were then held at the animal care facility at the University of Calgary. The ground squirrels were caged with free access to food and water at 22°C for 8 weeks on a natural autumn photoperiod (10 h light: 14 h dark). Following this period, half of the animals were sampled as control (euthermic) and the other half of the animals were moved to dark room maintained at 4°C with water, but no food (hibernating). Subsequently, animals from these conditions were sampled after 2 days of continuous torpor (rectal temperature 5−8°C). Both hibernating and euthermic animals were killed by decapitation and tissues were immediately excised, frozen in liquid nitrogen, and then stored at -80°C. All protocols described above for animal holding and hibernation had prior approval by the university animal care committee and met guidelines for the Canadian Council on Animal Care. The protocols used for care and handling of Richardson's ground squirrels, *U. richardsonii*, were reported previously [15, 16].

2.2 Preparation of tissue extracts

Samples of frozen skeletal muscle tissue of *U. richardsonii* were homogenized in a 1:10 w:v in ice cold homogenization buffer A (25 mM K_2PO_4, 2 mM EDTA, 2 mM EGTA, 15 mM β-glycerophosphate, 10 mM β-mercaptoethanol, 10% v:v glycerol, pH 6.0) in addition to a few crystals of phenylmethylsulphonyl fluoride (PMSF). Samples were homogenized using a Polytron homogenizer (Brinkmann Instruments, Westbury, NY, USA) and centrifuged in a pre-chilled Eppendorf 5810 R tabletop centrifuge (22331 Hamburg, GER) for 30 min at 13,500 × g (4°C). The supernatant (crude homogenate) was collected and held on ice until further use.

2.3 NADP-isocitrate dehydrogenase purification

Crude skeletal muscle homogenate was initially applied to a CM⁻ Sephadex column previously equilibrated with 30 mL of buffer A. Unbound protein was removed from the column with 30 mL wash of buffer A. The enzyme was then eluted from the column with a 20 mL bump of 45 mM isocitrate solution made in buffer A. Using an automated fraction collector (Gilson Medical Electronics, Inc., Middleton, WI,

USA), 1.6 mL fractions of column eluant were collected. From each fraction, 10 μL was taken and assayed for NADP-IDH activity. Peak activity fractions were pooled together, increased to pH 7.0 and diluted 10:1 v:v with buffer B (25 mM imidazole, 2 mM EDTA, 2 mM EGTA, 15 mM β-glycerophosphate 10 mM β-mercaptoethanol, 10% v:v glycerol, pH 7.0). The diluted sample was then applied to a Cibacron blue column that had been previously equilibrated with 30 mL of buffer B. NADP-IDH was eluted with $0-2$ M KCl gradient made in buffer B and collected in 1.6 mL fractions. Aliquots of 10 μL were taken to access NADP-IDH activity from each fraction. Fractions with the highest activity were pooled together. The salt was subsequently removed from the final sample with use of the Sephadex G-25 medium (Cat# G25150-10G, Sigma-Aldrich). For every 500 μL of enzyme sample, 5 mL of beads equilibrated with 5 mL of buffer B were used and centrifuged at 12, 500 x g for 1 min. The final sample was held at 4°C until further use. This procedure was observed for both euthermic and hibernating samples. Protein concentrations were determined using Coomassie blue G-250 dye-binding reagent (Bio-Rad, Hercules, CA, USA) as instructed by the manufacturer using bovine serum albumin as a standard [17] .

2.4 NADP-isocitrate dehydrogenase enzyme assay

NADP-IDH activity was measured as the rate of production of NADH by measuring absorbance at 340 nm using a Multiskan spectrophotometer (Thermo Scientific, Waltham, MA, USA). Optimal assay conditions were found to be 35 mM Tris (pH 7.2), 2.5 mM isocitrate, 0.8 mM NADP, 0.5 mM Mg^{2+}, and 10 μL of purified enzyme in a 200 μL total volume. Assays were initiated through the addition of NADP, and assays were run at room temperature (22°C). For kinetic analysis, K_m values for NADP, isocitrate and Mg^{2+} were determined at constant, saturating co-substrate concentrations. I_{50} values were determined by the addition of increasing concentration of denaturant molecules (urea, KCl) to the purified enzyme. The kinetic analysis of all three substrate's K_m values was also performed at 4°C to simulate hibernating temperature conditions. Kinetic data were analyzed using the Kinetics v.3.5.1 program [18].

2.5 Gel electrophoresis and staining

Purified NADP-IDH samples were separated on 10% SDS-PAGE gels via electrophoresis for 55 minutes at 180 V. Gels were then stained by Coomassie Blue dye (0.25% w:v brilliant blue R, 7.5% v:v acetic acid, 50% v:v methanol) for 1 hour. Adequately stained gels were then immersed in destain solution (10% v:v acetic acid, 25% v:v methanol) until distinct bands were visualized. Gels were then visualized and imaged using a ChemiGenius Bio-Imaging system with GeneSnap software (Syngene, Frederick, MD).

2.6 Western blotting

Skeletal muscle NADP-IDH PTMs were analyzed using Western blotting. In brief, samples of purified NADP-IDH were concentrated 8× using an Amicon® Ultra Filter Centricon (Millipore). For both euthermic and hibernating preparations, concentrated samples were mixed 1:1 (v:v) with SDS loading buffer (100 mM Tris buffer [pH 6.8], 4% w:v SDS, 20% v:v glycerol, 0.2% w:v bromophenol blue, and 10% v:v 2-mercaptoethanol) and boiled for 5 minutes. SDS resolving gel (10% v:v acrylamide, 400 mM Tris [pH 8.8], 0.1% w:v SDS, 0.2% w:v ammonium persulfate [APS], 0.04% v:v TEMED) were prepared with 5% stacking gel (5% acrylamide, 190 mM Tris [pH 6.8], 0.1% w:v SDS, 0.15% w:v APS, 0.1% v:v TEMED). Samples were

loaded onto these gels and separated electrophorectically in SDS-PAGE running buffer (25 mM Tris [pH 8.5], 190 mM glycine, and 0.1% w:v SDS) for 45 minutes at 180 V. Following electrophoresis, proteins on the gel were electroblotted onto polyvinylidene difluoride (PVDF) membranes (Millipore) by wet transfer for 90 minutes at 160 amps.

After protein transfer, PVDF membranes were washed three times with Tris buffered saline (TBS; 100 mM Tris, 140 mM NaCl [pH 7.6]) containing 0.05% Tween-20 (TBST) for 5 minutes each wash. Following this initial washing, membranes were blocked for 10 minutes with 2.5% skim milk before primary antibodies (diluted 1:1000 v:v in TBST) were applied for overnight incubations at 4°C on a rocker. Primary antibodies included: (1) rabbit anti-phosphoserine (Cat. #618100, Invitrogen, Carlsbad, CA, USA); (2) rabbit anti-phosphothreonine (Cat. #718200, Invitrogen, Carlsbad, CA, USA); (3) mouse anti-phosphotyrosine (Cat. #615800, Invitrogen, Carlsbad, CA, USA). Following primary antibody incubation, membranes were washed three times with TBST for 5 minutes each and incubated with either a 1:8000 v:v dilution of goat anti-rabbit IgG-peroxidase secondary antibody (Cat. #APA007P, BioShop Canada Inc., Burlington, ON, Canada) or 1:8000 v:v dilution of anti-mouse IgG-peroxidase secondary antibody (Cat. #APA005P.2, BioShop Canada Inc., Burlington, ON, Canada) depending on the primary antibody. All phospho-antibody probed membranes were incubated in their respective secondary antibody dilution for 40 minutes at room temperature. Blots were washed with TBST (3 x 5min) prior to visualization on the ChemiGenius Bioimaging System (Syngene, Frederick, MD, USA). Observed band intensities were quantified using the GeneTools software (Syngene, Frederick, MD, USA). Subsequent staining of visualized membranes in Coomassie blue occurred in order to standardize immunoblot band intensities.

2.9 Bioinformatics

The NADP-IDH sequence of the 13-lined ground squirrel, *Ictidomys tridecemlineatus* was taken as it is the closest sequenced relative of the Richardson's ground squirrel. For determination of molecular weight and isoelectric point, the ExPASy Compute pI/Mw bioinformatics tool was used (http://web.expasy.org/compute_pi/). ClustalW2 was used to observe the conservation of NADP-IDH amino acid residues across different animals (https://www.ebi.ac.uk/Tools/msa/clustalw2/). The NADP-IDH sequence from *I. tridecemlineatus* was aligned with rabbit (*Oryctolagus cuniculus)*, humans *(Homo sapiens)* that do not undergo hibernation and frog (*Xenopus laevis*) that can experience significant dehydration stress (Larkin et al., 2007). Potential phosphorylation sites on the NADP-IDH amino acid sequence were predicted using NetPhos 3.1 server (https://services.healthtech.dtu.dk/service.php?NetPhos-3.1) [19]. Finally, protein structure of NADP-IDH was predicted using SWISS-MODEL (https://swissmodel.expasy.org/), a protein structure homology-modelling server [20–22].

2.10 Data and statistical analysis

All enzyme assays were analyzed using a Microplate analysis program (MPA) [23], while kinetic parameters were determined using a nonlinear least squares regression computer program Kinetics v.3.5.1 [18]. RBioplot statistical software was used in data analysis to generate graphs and perform

Student's t-test or analysis of variance (ANOVA) combined with a Tukey's post-hoc test [24]. Data was determined to be statistically different between euthermic and torpid groups when the p < 0.05.

3. Results

3.1 Purification of NADP-IDH from the skeletal muscle of euthermic and hibernating U. richardsonii

NADP-IDH was successfully purified from skeletal muscle of euthermic and hibernating *U. richardsonii*. Purification was performed by two chromatography steps in succession: (1) CM⁻ column (enzyme eluted via isocitrate bump), and (2) a Cibacron blue affinity column (elution with 0-2M KCl) (Table 1). Elution of the euthermic and hibernating NADP-IDH from the CM⁻ Sephadex column resulted in a 3.2- and 6-fold purification respectively (Table 1). Finally, elution of the euthermic and hibernator enzyme from the Cibacron blue column using a KCl gradient resulted in a 5.9- and 8.8-fold purification respectively (Table 1). The final purification resulted in specific activities of 0.84 U/mg for euthermic NADP-IDH and 0.61 U/mg, for hibernator NADP-IDH (Table 1). SDS-PAGE and Coomassie Blue was used to visually assess the purification of NADP-IDH. The purified enzyme had a molecular weight of ⯑46 kDa (Fig. 1).

Table 1
Typical purification and yield of Richardson's ground squirrels (*Urocitellus richardsonii*) NADP-IDH from skeletal muscle of euthermic and hibernating ground squirrels.

Step	Total protein (mg)	Total activity (U)	Specific activity (U/mg)	Fold purification	Yield (%)
Euthermic					
Crude	14.8	2.08	0.14	-	-
CM Sephadex	2.10	0.96	0.46	3.2	46.2
Cibacron Blue	0.59	0.49	0.84	5.9	23.6
Hibernating					
Crude	22.5	1.56	0.069	-	-
CM Sephadex	1.76	0.74	0.42	6.0	47.3
Cibacron Blue	0.58	0.36	0.61	8.8	22.9

3.2 Kinetic parameters of purified NADP-IDH from euthermic and hibernating skeletal muscle

Multiple kinetic parameters of purified skeletal muscle NADP-IDH were compared between euthermic and hibernating states (Table 2). There were significant differences in the Km values for isocitrate between euthermic and hibernating ground squirrel at 22°C and 5°C. The Km values for isocitrate and NADP at 22°C for the hibernating form was decreased by ⬚85% (5.5 ± 0.6 µM) and by ⬚83% (1.2 ± 0.1 µM) respectively from their respective euthermic values. Following the above trend, the Km value for NADP at 5°C showed a decrease of ⬚74% (3.6 ± 0.4 µM) compared to euthermic value of NADP-IDH (14 ± 3 µM) at 5°C. Interestingly, at 5°C Km value for isocitrate showed 4-fold increase in hibernating form (24 ± 3 µM) of NADP-IDH as compared to its euthermic NADP-IDH (6 ± 0.4 µM). The Km Mg^{2+} values at 22°C and 5°C showed ⬚2-fold (19 ± 0.8 µM) and ⬚ 3-fold (81 ± 4 µM) increase respectively in hibernating form of NADP-IDH as compared to their corresponding euthermic values (Table 2). The effects of inhibition by general enzyme denaturants were determined for euthermic and hibernating NADP-IDH at standard conditions (pH 7.2, 22°C). A significant increase in KCl I$_{50}$ values was observed in hibernating NADP-IDH (0.85 ± 0.01 M) when compared to the corresponding euthermic value (0.68 ± 0.04 M) (Table 2). No significant differences were observed between euthermic (4.21 ± 0.08 M) and hibernating (4.54 ± 0.16 M) urea I$_{50}$ values (Table 2).

Table 2

Comparison of the kinetic parameters of purified muscle NADP-IDH from euthermic and hibernating Richardson's ground squirrels (*Urocitellus richardsonii*). Data are means ± SEM, n = 6. "a" indicates a significant difference from the corresponding euthermic condition (Student's *t* test, two-tailed, *p* < 0.05). "b" indicates a significant difference from corresponding hibernating value at 22°C and 5°C.

Enzyme parameters	Euthermic	Hibernating
Forward reaction (isocitrate to α-ketoglutarate) at 22°C	36 ± 5	5.5 ± 0.6^a
K$_m$, isocitrate, pH 7.2 (µM)	7.2 ± 0.5	1.2 ± 0.1^a
K$_m$, NADP, pH 7.2 (µM)	9.6 ± 0.3	19 ± 0.8 ^{a}
K$_m$, Mg^{2+}, pH 7.2 (µM)	0.68 ± 0.04 4.21 ± 0.08	0.85 ± 0.01^a
I$_{50}$, KCl, pH 7.2 (M)		4.54 ± 0.16
I$_{50}$, urea, pH 7.2 (M)	6 ± 0.4	24 ± 3^{ab}
Forward reaction (isocitrate to α-ketoglutarate) at 5°C	14 ± 3	3.6 ± 0.4^{ab}
K$_m$, isocitrate, pH 7.2 (µM)	26 ± 4	81 ± 4^{ab}
K$_m$, NADP, pH 7.2 (µM)		
K$_m$, Mg^{2+}, pH 7.2 (µM)		

3.3 Reversible post-translational modifications of skeletal muscle NADP-IDH.

Immunoblotting was used to assess differences in post-translational phosphorylation on euthermic and hibernating NADP-IDH enzyme. Overall phosphorylation of threonine and serine residues of the hibernating NADP-IDH enzyme increased 3.7- and 4.6-fold respectively when compared to the corresponding euthermic enzyme (Fig. 2).

3.4 Bioinformatic analysis

Analysis of the predicted 13-LGS NADP-IDH amino acid sequence (NCBI Reference Sequence: XP_005342105.1) via the phosphorylation site predict server NetPhos3.1 (https://services.healthtech.dtu.dk/service.php?NetPhos-3.1) [19] indicated 18 threonine, 21 serine and 10 tyrosine sites (Fig. 3). The isoelectric point (pI) and molecular weight of the enzyme were determined to be 6.34 and 46.46kDa, respectively. Sequence alignments between *I. tridecemlineatus*, human, rabbit, and frog NADP-IDH was determined. With respect to the primary structure of the enzyme, the amino acid sequence seems to be highly conserved across mammals (squirrels, human and rabbit) (Fig. 4). Finally, SWISS-MODEL was used to generate NADP-IDH structure (Fig. 5).

4. Discussion

Various metabolic adaptations and regulatory controls are required to withstand metabolic rate depression, including reorganization of metabolic fuel and differential expression of genes/proteins [25]. Most importantly, and of particular interest to this study, are the ways in which mammals coordinate their entry into arousal from torpor and sustain its metabolic function at low body temperature without causing hypothermia. Huge reserves of triglycerides act as a primary fuel for most organs during hibernation. Strict metabolic rate depression and allowing the body temperature to fall to near ambient temperatures during torpor bouts, allows hibernators to save huge amounts of energy as compared to euthermic animals (Ruf & Geiser, 2015). Richardson's ground squirrel is additionally faced with oxidative stress during hibernation, particularly during arousals in which oxygen consumption increases drastically [9, 27]. In many instances of hypometabolism, an increase in antioxidant enzyme activity is observed to prepare for imminent oxidative stress upon arousal and preserve current cell integrity during periods of reduced repair [28–31]. NADP-IDH often contributes significantly to the NADPH pool required for reductive fatty acid biosynthesis. This enzyme provides NADPH for maintenance of proper oxidation-reduction balance and protection against oxidative damage [32].

NADP-IDH was purified to electrophoretic homogeneity from Richardson's ground squirrel skeletal muscle through a combination of ion-exchange and affinity chromatography (Fig. 1). The apparent molecular weight (~ 46 kDa) determined by SDS-PAGE corresponds well with the molecular weights reported for the same enzyme through bioinformatics analysis. Kinetic analysis of NADP-IDH was assessed at high and low temperatures. Many significant changes in parameters were observed when comparing euthermic and hibernating samples. The Km values of isocitrate and NADP were both significantly reduced in hibernating squirrels at 22°C as compared to euthermic control squirrels (Table 2). A decrease in K_m values is suggestive of an increased enzyme affinity and, in turn, enzyme activity in the hibernating state. Increased enzyme activity is indicative of elevated NADPH production in hibernating squirrels. This

increased NADPH presence could contribute to enhanced antioxidant activity and overall oxidative stress defense in the organism while in the hypometabolic state. Previous studies done by Vucetic et al., 2013 [33], on the impact of hibernation on antioxidant defences in the European ground squirrel (*Spermophilus citellus*) showed increase in antioxidant defence enzyme protein expressions in the hibernating state. Similar study was also done by Allan & Storey on a molecular level, in which they analysed the expression downstream antioxidant target, NF-κB in skeletal muscle of hibernating ground squirrels (*Ictidomys tridecemlineatus*) [34]. During hibernation, the expression of NF-κB was increased, particularly in early torpor and arousal suggesting increased antioxidant defense [34]. Additionally, in this study, increased expression of manganese dependent superoxide dismutase in early torpor and increased expression of heme oxygenase 1 in early arousal was also noted [34]. One more study suggested that there was a significant increase in MafK affirming an increase in relative Nrf2 and catalase levels seen in arousal. These results seen during arousal correspond to a surge in oxygen consumption, which causes increased reactive oxygen species production[31]. Overall, this is also contributing to the idea that ground squirrels increase oxidative stress defense during hibernation to cope with increased oxygen fluctuations during periodic arousals and to preserve cells during reduced repair periods in hypometabolism.

Interestingly, when observing the same K_m kinetic parameters at a reduced temperature (5°C), the increase in enzyme affinity in the hibernating state is no longer observed. In fact, both isocitrate and Mg^{2+} K_m values were increased in the hibernating state when compared to their respective euthermic counterparts (Table 2). Such results are more indicative of a decrease in enzyme affinity in the hibernating state at the cooler temperature. Perhaps, reduced NADP-IDH activity in the hibernating state would allow energy conservation in ground squirrels during hypometabolism. Reduced metabolic rate and the suppression of unnecessary processes during stages of reduced oxygen, food, and water consumption has been well studied in the past [8, 35, 36]. In hibernators, evidence has been presented that global suppression of ATP expensive processes such as transcription, translation, and growth stimulated by the Akt transcription factor takes place in order to facilitate energy conservation during hibernation [37–39]. Therefore, decreased activity of NADP-IDH in ground squirrel skeletal muscle at reduced temperatures could be the result of an assortment of energy conservation mechanisms. The conflicting results of K_m values of NAP-IDH at 22°C and 5°C are indicative of more complex regulation of this enzyme. During hibernation, the ground squirrel reduces its core body temperature to near ambient temperatures and can remain at approximately 5°C for prolonged bouts of torpor [2]. However, the squirrels do not always remain in a state of torpor throughout hibernation and instead cycle back to normal body temperature and metabolic rate periodically through interbout arousal periods [4, 9]. During torpor at colder temperatures, there is a decrease in oxidative stress. When moving to periods of arousal, the immediate phase of high oxygen consumption puts the hibernating squirrel at risk of increased mitochondrial reactive oxygen species (ROS) production [27, 40]. Thus, enzyme activity is likely being controlled in Richardson's ground squirrel based on antioxidant need by regulating NADP-IDH not only according to euthermic or hibernating state, but also according to temperature. Altogether, this study explored the idea that at low temperatures, when oxidative stress is low and energy conservation needs are high, NADP-IDH can be downregulated. Yet, at increased temperatures and increased ROS threat during interbout arousal periods, NADPH production

becomes more essential to cell survivability and is thus upregulated. Previous studies of enzymes from ground squirrels have also documented significant changes in the kinetic properties of enzymes in hibernating versus euthermic states and in high versus low assay temperatures. These include creatine kinase [41], hexokinase [42], pyruvate kinase [43] and citrate synthase [44] (all well-known regulatory enzymes) from skeletal muscle of Richardson's ground squirrels. A significant increase in I_{50} value of KCl at room temperature was observed in hibernating as compared to euthermic squirrel (Table 2). Increased KCl tolerance could mean that the hibernating form of NADP-IDH has increased chemical stability in Richardson's ground squirrels. A similar phenomenon was observed in the SERCA (sarcoendoplasmic reticulum Ca^{2+}-ATPase) enzyme of turtles which undergoes anoxia, another form of hypometabolic stress [45].

The differences observed in the kinetic properties of NADP-IDH purified from euthermic and hibernating skeletal muscles may be explained by structural differences. Phosphorylation levels of serine, threonine, and tyrosine residues were therefore assessed by western blotting. There was a significant increase in phosphorylation on serine and threonine residues of NADP-IDH in the hibernating ground squirrels (Fig. 2). Reversible protein phosphorylation has been known to control the activity of key metabolic enzymes during hibernation in Richardson's ground squirrel in earlier studies. A study done by Bell & Storey showed skeletal muscle pyruvate kinase of hibernating ground squirrel, *U. richardsonii* was regulated post-translationally [43]. They indicated that skeletal muscle pyruvate kinase from the hibernating animal was significantly more phosphorylated [43]. In another study, immunoblotting showed that hibernator muscle glycerol-3-phosphate dehydrogenase had a higher phosphoserine content than in euthermic controls [3, 46]. Protein phosphorylation is an important post-translational modification that can quickly and reversibly alter the properties of metabolic enzymes [47]. Phosphorylation of NADP-IDH during hibernation could thus also be responsible for the kinetic differences observed in the present study.

To complement the experimental studies on *U. richardsonii* NADP-IDH, bioinformatics tools were used to analyze the NADP-IDH protein sequence from the thirteen-lined ground squirrel, a closely related hibernator with a sequenced genome (Fig. 3). This analysis was aimed at identifying sites of post-translational modifications that may play a role in stabilizing enzyme structure and enhancing enzyme functionality in euthermic versus hibernating states. Bioinformatics results further confirmed the presence of potential threonine and serine residues which can likely be phosphorylated in hibernating NADP-IDH enzyme. (Fig. 3). The addition of phosphate groups to these serine or threonine amino acid residues could play a role in modifying ground squirrel skeletal muscle functionality at high (euthermic) versus low (hibernating) body temperatures.

5. Conclusion

Therefore, this study demonstrates the regulation of the NADP-IDH in euthermic and hibernating Richardson's ground squirrel. Purified NADP-IDH exhibited distinct kinetic properties in response to hibernation compared to the enzyme purified from euthermic animals. These differences are likely due to the phosphorylation of hibernating form NADP-IDH. The hibernating form of NADP-IDH from the skeletal

muscles of Richardson's ground squirrels maintain better functionality at 22°C than 5°C when compared to their respective euthermic NADP-IDH. In high temperature hibernation periods (i.e., interbout arousals), the increased influx of oxygen could lead to increased threat of ROS damage, leading to increased NADP-IDH activity to mitigate resultant oxidative damage. However, in low temperature hibernation conditions and subsequently low oxidative damage periods, energy conversation is favoured and NADP-IDH activity is decreased accordingly. The data presented here in reinforce the fact that small hibernators such as Richardson's ground squirrels are confronted with oxidative stress over torpor-arousal cycles and must up-regulate their antioxidant defenses to prevent oxidative injuries whenever required.

Declarations

Conflicts of Interest: The authors declare no conflict of interest.

Data Availability: The data are available on reasonable request.

Ethics approval: All protocols for animal care and treatment had prior approval by the Carleton University Animal Care Committee and met guidelines for the Canadian Council on Animal Care.

Author Contributions: IAM and KBS conceptualized and designed the project and IAM conducted all experiments. Data analysis and assembly of the manuscript were carried out by AV, IAM , and KBS.

References

1. Lyman CP, Willis JS, Malan A, Wang LCH (1984)Hibernation and Torpor in Mammals and Birds
2. Abnous K, Dieni CA, Storey KB (2008) Regulation of Akt during hibernation in Richardson's ground squirrels. Biochim Biophys Acta - Gen Subj 1780:185–193. https://doi.org/10.1016/j.bbagen.2007.10.009
3. Ruberto AA, Childers CL, Storey KB (2016) Purification and properties of glycerol-3-phosphate dehydrogenase from the liver of the hibernating ground squirrel, *Urocitellus richardsonii*. Comp Biochem Physiol Part B Biochem Mol Biol 202:48–55. https://doi.org/10.1016/j.cbpb.2016.08.001

4. Wang LCH (1979) Time patterns and metabolic rates of natural torpor in the Richardson's ground squirrel. Can J Zool 57:149–155. https://doi.org/10.1139/z79-012

5. Landau BR, Dawe AR (1958) Respiration in the Hibernation of the 13-Lined Ground Squirrel. Am J Physiol Content 194:75–82. https://doi.org/10.1152/ajplegacy.1958.194.1.75

6. Buck CL, Barnes BM (2000) Effects of ambient temperature on metabolic rate, respiratory quotient, and torpor in an arctic hibernator. Am J Physiol Regul Integr Comp Physiol 279:R255–R262. https://doi.org/10.1152/ajpregu.2000.279.1.R255

7. Wang LCH, Lee TF (1996) Torpor and Hibernation in Mammals: Metabolic, Physiological, and Biochemical Adaptations. In: Comprehensive Physiology. Wiley, pp 507–532

8. Storey KB (1997) Metabolic regulation in mammalian hibernation: enzyme and protein adaptations. Comp Biochem Physiol A Physiol 118:1115–1124. https://doi.org/10.1016/s0300-9629(97)00238-7

9. Carey HV, Andrews MT, Martin SL (2003) Mammalian hibernation: cellular and molecular responses to depressed metabolism and low temperature. Physiol Rev 83:1153–1181. https://doi.org/10.1152/physrev.00008.2003

10. Storey KB, Storey JM (2004) Metabolic rate depression in animals: transcriptional and translational controls. Biol Rev Camb Philos Soc 79:207–233. https://doi.org/10.1017/s1464793103006195

11. Brooks SP, Storey KB (1992) Mechanisms of glycolytic control during hibernation in the ground squirrel *Spermophilus lateralis*. J Comp Physiol B 162:23–28. https://doi.org/10.1007/BF00257932

12. MacDonald JA, Storey KB (1998) cAMP-dependent protein kinase from brown adipose tissue: temperature effects on kinetic properties and enzyme role in hibernating ground squirrels. J Comp Physiol B 168:513–525. https://doi.org/10.1007/s003600050172

13. Xu X, Zhao J, Xu Z et al (2004) Structures of human cytosolic NADP-dependent isocitrate dehydrogenase reveal a novel self-regulatory mechanism of activity. J Biol Chem 279:33946–33957. https://doi.org/10.1074/jbc.M404298200

14. Ju H-Q, Lin J-F, Tian T et al (2020) NADPH homeostasis in cancer: functions, mechanisms and therapeutic implications. Signal Transduct Target Ther 5:231. https://doi.org/10.1038/s41392-020-00326-0

15. Thatcher BJ, Storey KB (2001) Glutamate dehydrogenase from liver of euthermic and hibernating Richardson's ground squirrels: evidence for two distinct enzyme forms. Biochem Cell Biol 79:11–19. https://doi.org/10.1139/o00-086

16. Bell RAV, Dawson NJ, Storey KB (2012) Insights into the In Vivo Regulation of Glutamate Dehydrogenase from the Foot Muscle of an Estivating Land Snail. Enzyme Res 2012:1–10. https://doi.org/10.1155/2012/317314

17. Bradford MM (1976) A rapid and sensitive method for the quantitation of microgram quantities of protein utilizing the principle of protein-dye binding. Anal Biochem Volume 72,:248–254. https://doi.org/10.1016/0003-2697(76)90527-3

18. Brooks SPJ (1992) A simple computer program with statistical tests for the analysis of enzyme kinetics. Biotechniques 13(6):906–911

19. Blom N, Gammeltoft S, Brunak S (1999) Sequence and structure-based prediction of eukaryotic protein phosphorylation sites. J Mol Biol 294:1351–1362. https://doi.org/10.1006/jmbi.1999.3310

20. Arnold K, Bordoli L, Kopp J, Schwede T (2006) The SWISS-MODEL workspace: a web-based environment for protein structure homology modelling. Bioinformatics 22:195–201. https://doi.org/10.1093/bioinformatics/bti770

21. Bordoli L, Kiefer F, Arnold K et al (2009) Protein structure homology modeling using SWISS-MODEL workspace. Nat Protoc 4:1–13. https://doi.org/10.1038/nprot.2008.197

22. Biasini M, Bienert S, Waterhouse A et al (2014) SWISS-MODEL: modelling protein tertiary and quaternary structure using evolutionary information. Nucleic Acids Res 42:W252–W258. https://doi.org/10.1093/nar/gku340

23. Brooks SPJ (1994) A program for analyzing enzyme rate data obtained from a microplate reader. Biotechniques 17(6):1154–1161

24. Zhang J, Storey KB (2016) RBioplot: an easy-to-use R pipeline for automated statistical analysis and data visualization in molecular biology and biochemistry. PeerJ 4:e2436. https://doi.org/10.7717/peerj.2436

25. Storey KB (2003) Mammalian hibernation. Transcriptional and translational controls. Adv Exp Med Biol 543:21–38

26. Ruf T, Geiser F (2015) Daily torpor and hibernation in birds and mammals. Biol Rev 90:891–926. https://doi.org/10.1111/brv.12137

27. Orr AL, Lohse LA, Drew KL, Hermes-Lima M (2009) Physiological oxidative stress after arousal from hibernation in Arctic ground squirrel. Comp Biochem Physiol A Mol Integr Physiol 153:213–221. https://doi.org/10.1016/j.cbpa.2009.02.016

28. Storey KB, Storey JM (2012) Aestivation: signaling and hypometabolism. J Exp Biol 215:1425–1433. https://doi.org/10.1242/jeb.054403

29. Krivoruchko A, Storey KB (2015) Turtle anoxia tolerance: Biochemistry and gene regulation. Biochim Biophys Acta - Gen Subj 1850:1188–1196. https://doi.org/10.1016/j.bbagen.2015.02.001

30. Moreira DC, Venancio LPR, Sabino MACT, Hermes-Lima M (2016) How widespread is preparation for oxidative stress in the animal kingdom? Comp Biochem Physiol Part A Mol Integr Physiol 200:64–78. https://doi.org/10.1016/j.cbpa.2016.01.023

31. Tessier SN, Breedon SA, Storey KB (2021) Modulating Nrf2 transcription factor activity: Revealing the regulatory mechanisms of antioxidant defenses during hibernation in 13-lined ground squirrels. Cell Biochem Funct 39:623–635. https://doi.org/10.1002/cbf.3627

32. Zera AJ, Newman S, Berkheim D et al (2011) Purification and characterization of cytoplasmic NADP+-isocitrate dehydrogenase, and amplification of the NADP+-IDH gene from the wing-dimorphic sand field cricket, *Gryllus firmus*. J Insect Sci 11:53. https://doi.org/10.1673/031.011.5301

33. Vucetic M, Stancic A, Otasevic V et al (2013) The impact of cold acclimation and hibernation on antioxidant defenses in the ground squirrel (*Spermophilus citellus*). Free Radic Biol Med 65:916–924. https://doi.org/10.1016/j.freeradbiomed.2013.08.188

34. Allan ME, Storey KB (2012) Expression of NF-κB and downstream antioxidant genes in skeletal muscle of hibernating ground squirrels, *Spermophilus tridecemlineatus*. Cell Biochem Funct 30:166–174. https://doi.org/10.1002/cbf.1832

35. Morin P, Storey KB (2006) Evidence for a reduced transcriptional state during hibernation in ground squirrels. Cryobiology 53:310–318. https://doi.org/10.1016/j.cryobiol.2006.08.002

36. Frerichs KU, Smith CB, Brenner M et al (1998) Suppression of protein synthesis in brain during hibernation involves inhibition of protein initiation and elongation. Proc Natl Acad Sci 95:14511–14516. https://doi.org/10.1073/pnas.95.24.14511

37. Cai D, McCarron RM, Yu EZ et al (2004) Akt phosphorylation and kinase activity are down-regulated during hibernation in the 13-lined ground squirrel. Brain Res 1014:14–21. https://doi.org/10.1016/j.brainres.2004.04.008

38. Storey KB (2010) Out Cold: Biochemical Regulation of Mammalian Hibernation – A Mini-Review. Gerontology 56:220–230. https://doi.org/10.1159/000228829

39. Biggar Y, Storey KB (2014) Global DNA modifications suppress transcription in brown adipose tissue during hibernation. Cryobiology 69:333–338. https://doi.org/10.1016/j.cryobiol.2014.08.008

40. Brown JCL, Chung DJ, Belgrave KR, Staples JF (2012) Mitochondrial metabolic suppression and reactive oxygen species production in liver and skeletal muscle of hibernating thirteen-lined ground squirrels. Am J Physiol Regul Integr Comp Physiol 302:R15–28. https://doi.org/10.1152/ajpregu.00230.2011

41. Abnous K, Storey KB (2007) Regulation of skeletal muscle creatine kinase from a hibernating mammal. Arch Biochem Biophys 467:10–19. https://doi.org/10.1016/j.abb.2007.07.025

42. Abnous K, Storey KB (2008) Skeletal muscle hexokinase: Regulation in mammalian hibernation. Mol Cell Biochem 319:41–50. https://doi.org/10.1007/s11010-008-9875-5

43. Bell RAV, Storey KB (2018) Purification and characterization of skeletal muscle pyruvate kinase from the hibernating ground squirrel, *Urocitellus richardsonii*: potential regulation by posttranslational modification during torpor. Mol Cell Biochem 442:47–58. https://doi.org/10.1007/s11010-017-3192-9

44. Green SR, Storey KB (2021) Skeletal muscle of torpid Richardson's ground squirrels (*Urocitellus richardsonii*) exhibits a less active form of citrate synthase associated with lowered lysine succinylation. Cryobiology 101:28–37. https://doi.org/10.1016/j.cryobiol.2021.06.006

45. Ramnanan CJ, McMullen DC, Bielecki A, Storey KB (2010) Regulation of sarcoendoplasmic reticulum Ca2+-ATPase (SERCA) in turtle muscle and liver during acute exposure to anoxia. J Exp Biol 213:17–25. https://doi.org/10.1242/jeb.036087

46. Ruberto AA, Logan SM, Storey KB (2019) Temperature and serine phosphorylation regulate glycerol-3-phosphate dehydrogenase in skeletal muscle of hibernating Richardson's ground squirrels. Biochem Cell Biol 97:148–157. https://doi.org/10.1139/bcb-2018-0198

47. Storey KB, Storey JM (2005) Biochemical Adaptation to Extreme Environments. Integrative Physiology in the Proteomics and Post-Genomics Age. Humana Press, Totowa, NJ, pp 169–200

Figures
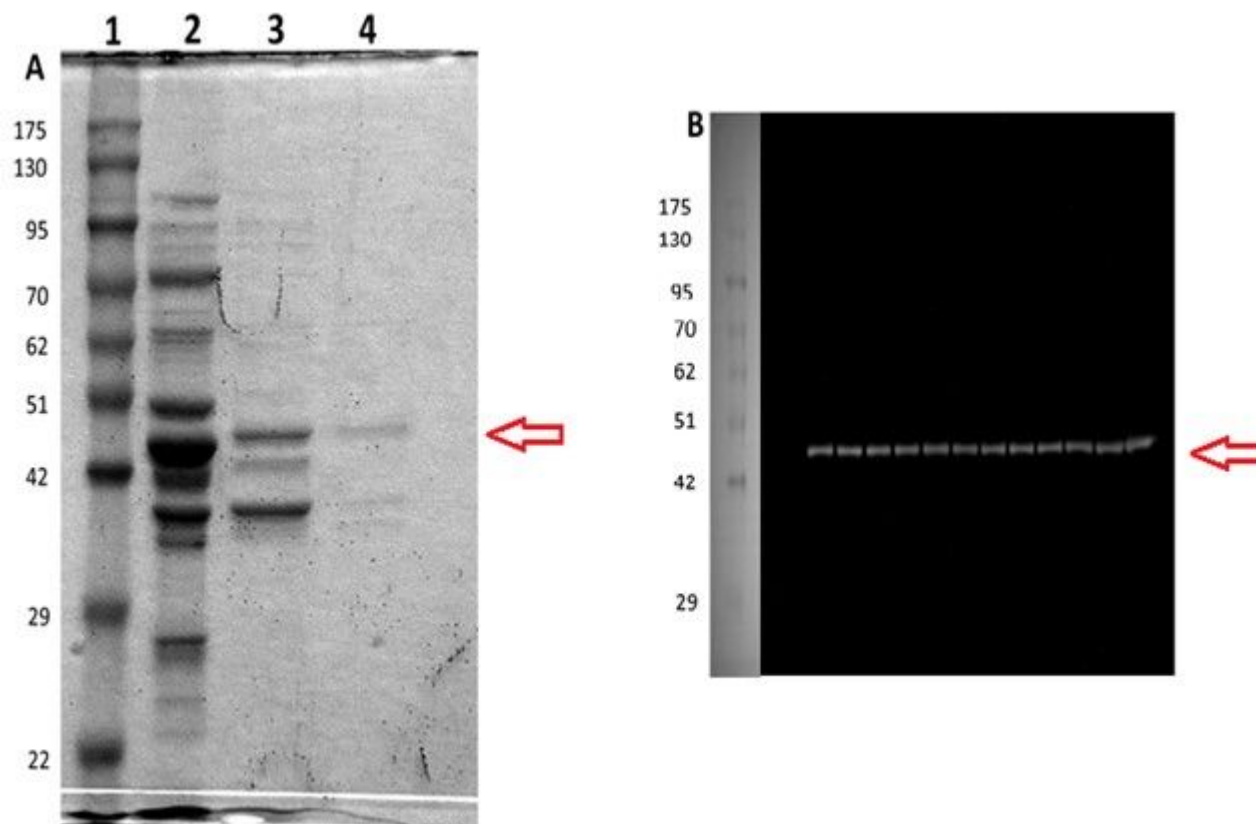
Figure 1

SDS-PAGE gel showing sample purification of skeletal muscle NADP-IDH from hibernating Richardson's ground squirrels. (A) Lanes are (1) protein ladder, (2) crude sample, (3) eluate from CM column, (4) and eluate from Cibacron blue column. Chemiluminescence ECL bands are additionally displayed demonstrating the immunoblotting results when probing for NADP-IDH with specific primary antibody. (B) The blot contains six replicates from the purified euthermic sample and six from the purified hibernating sample with the corresponding protein ladder displayed to the left for size referencing.

Figure 2

Quantification of post-translational modifications of purified euthermic and hibernating skeletal muscle NADP-IDH from *U. richardsonii*. Fold change in phosphorylation of purified enzyme samples is shown. Chemiluminescence signal intensities were standardized to protein amount, and the value for hibernating NADP-IDH was expressed relative to the control value that was set to 1. Data are mean ± SEM, n = 6 for

purified enzyme samples. * - indicates significant differences from the corresponding euthermic value determined by a student's *t*-test, $p < 0.05$.

A

```
XPPREDICTEDLXWQXALITYPRXTEINISXCITRATEDEHYDRXGENAS    #    50
ENADPCYTXPLASMICICTIDXMYSTRIDECEMLINEATXSMSQKIHGGS    #   100
VVEMQGDEMTRIIWELIKEKLIFPYVELDLHSYDLGIENSDATNDQVTKD    #   150
AAEAIKKYNVGIKCATITPDEKRVEEFKLKQMXKSPNGTIRNILGGTVFR    #   200
EAIICKNIPRLVSGWIKPIIIGRHAYGDQYRATDFVVPGPGKVEITYTPS    #   250
DGTQKVTYLVHNFEAGGGVAMGMYNEDKSIGDFAHSSFQMALSKGWPLYL    #   300
STKNTILKKYDGRFKDIFQEIYDKQYKSQFEAQKIWYEHRLIDDMVAQAM    #   350
KSEGGFIWACKNYDGDVQSDSVAQGYGSLGMMTSVLICPDGKTVEAEAAH    #   400
GTVTRHYRMYOKGOETSTNPIASIFAWTRGLAHRAKLDNNNELGIFAKAL    #   450
```

Figure 3

Predicted phosphorylation sites on threonine, serine, and tyrosine residues of NADP-IDH for thirteen lined ground squirrels (*I. tridecemlineatus*) as a reference for Richardson's ground squirrels. **(A)** Location of

predicted phosphorylation residues in the NADP-IDH sequence. In the above figure, a period (.) indicates the residue is predicted not to be phosphorylated as the score is below the threshold value (0.500). Residues with a score above threshold (0.500) that are predicted to be phosphorylated are denoted with either an S, T or Y. **(B)** Diagram depicting calculated scores for each residue in relation to the threshold line below.

```
X. laevis          MSKKINGGSVVEMQGDEMTRMIWDLIKEKLILPYVQLDLHSYDLGNENRDATDDQVTVDA
I. tridecemlineatus MSQKIHGGSVVEMQGDEMTRIIWELIKEKLIFPYVELDLHSYDLGIENSDATNDQVTKDA
O. cuniculus       MSKKIHGGSVVEMQGDEMTRIIWELIKEKLIVPYVELDLHSYDLGIENRDATNDQVTKDA
H. sapiens         MSKKISGGSVVEMQGDEMTRIIWELIKEKLIFPYVELDLHSYDLGIENRDATNDQVTKDA
                   **:**  **************:**:*******  ***:*********:** ***:**** **

X. laevis          AEAIKKYNVGIKCATITPDEKRVEEFNLKQMWKSPNGTIRNILGGTVFREAIICKNIPRL
I. tridecemlineatus AEAIKKYNVGIKCATITPDEKRVEEFKLKQMXKSPNGTIRNILGGTVFREAIICKNIPRL
O. cuniculus       AEAIKKYHVGVKCATITPDEKRVEEFKLKQMWKSPNGTIRNILGGTVFREAIICKNIPRL
H. sapiens         AEAIKKHNVGVKCATITPDEKRVEEFKLKQMWKSPNGTIRNILGGTVFREAIICKNIPRL
                   ******::**.*****************:**** ***************************

X. laevis          VSGWVKPIIIGRHAYGDQYRATDFVVPGPGKVEISFTPKDGGEAIKVVIHNFEDCGGVAL
I. tridecemlineatus VSGWIKPIIIGRHAYGDQYRATDFVVPGPGKVEITYTPSDGTQKVTYLVHNFEAGGGVAM
O. cuniculus       VTGWVKPIIIGRHAYGDQYRATDFVVPGPGKVEITYTPSDGTQKVTYLVHNFEEGGGVAM
H. sapiens         VSGWVKPIIIGRHAYGDQYRATDFVVPGPGKVEITYTPSDGTQKVTYLVHNFEEGGGVAM
                   *:**:*****************************::**.**  : :.*::**** ****:

X. laevis          GMYNTDQSIKDFAHSSFQMALSKSWPLYMSTKNTILKRYDGRFKDIFQEIYEKEVKSQFE
I. tridecemlineatus GMYNEDKSIGDFAHSSFQMALSKGWPLYLSTKNTILKKYDGRFKDIFQEIYDKQYKSQFE
O. cuniculus       GMYNQDKSIEDFAHSSFQMALSKGWPLYLSTKNTILKKYDGRFKDIFQEIYDKQYKSQFE
H. sapiens         GMYNQDKSIEDFAHSSFQMALSKGWPLYLSTKNTILKKYDGRFKDIFQEIYDKQYKSQFE
                   **** *:** ************** ****:********:************:*:.******

X. laevis          EQKIWYEHRLIDDMVAQAMKSEGGFIWACKNYDGDVQSDSVAQGYGSLGMMTSVLICPDG
I. tridecemlineatus AQKIWYEHRLIDDMVAQAMKSEGGFIWACKNYDGDVQSDSVAQGYGSLGMMTSVLICPDG
O. cuniculus       AQKIWYEHRLIDDMVAQAMKSEGGFIWACKNYDGDVQSDSVAQGYGSLGMMTSVLICPDG
H. sapiens         AQKIWYEHRLIDDMVAQAMKSEGGFIWACKNYDGDVQSDSVAQGYGSLGMMTSVLVCPDG
                   *********************************************************:****

X. laevis          KTVEAEAAHGTVTRHYRMHQKGQETSTNPIASIFAWSRGLDHRATLDNNQELKNFATALE
I. tridecemlineatus KTVEAEAAHGTVTRHYRMYQKGQETSTNPIASIFANTRGLAHRAKLDNNELGIFAKALE
O. cuniculus       KTVEAEAAHGTVTRHYRMHQKGQETSTNPIASIFAWTRGLAHRAKLDNNKELSFFANALE
H. sapiens         KTVEAEAAHGTVTRHYRMYQKGQETSTNPIASIFAWTRGLAHRAKLDNNKELAFFANALE
                   *****************:.*****************.*** ***.****:** **.***

X. laevis          EVCIETIEAGYMTKDLAACIKGLPNVQRSDYLNTFEFMDKLAENLQLKLAVFPKL
I. tridecemlineatus DVCIETIEAGFMTKDLAACIKGLPNVQRSDYLNTFEFMDKLGENLKIKLAQAKL-
O. cuniculus       EVCIETIEAGFMTKDLAACIKGLPNVQRSDYLNTFEFMDKLGENLKIKLSDAKL-
H. sapiens         EVSIETIEAGFMTKDLAACIKGLPNVQRSDYLNTFEFMDKLGENLKIKLAQAKL-
                   :*.*******:********************************.***::**::**:
```

Figure 4

Multiple alignment of the deduced amino acid sequence of thirteen lined ground squirrels (*I. tridecemlineatus*) as a reference for Richardson's ground squirrels. Comparison of sequence is to three non-hibernating organisms, two mammals (rabbit and human) and one amphibian. Asterisks (*) denote amino acid residues that are conserved amongst all species; colons (:) denote the conversion between amino acid residues of strongly similar properties; periods (.) denote the conversion between residues of weakly similar properties. Additionally, amino acid differences from the *I. tridecemlineatus* sequence are

highlighted for each the frog (blue), rabbit (red) and human (green) sequences. Amino acid residues unique to only ground squirrels are highlighted in orange boxes. Accession numbers for the frog, rabbit and human NADP-IDH sequences are XP_018094513.1, XP_017198555.1 and NP_001269316.1 respectively.
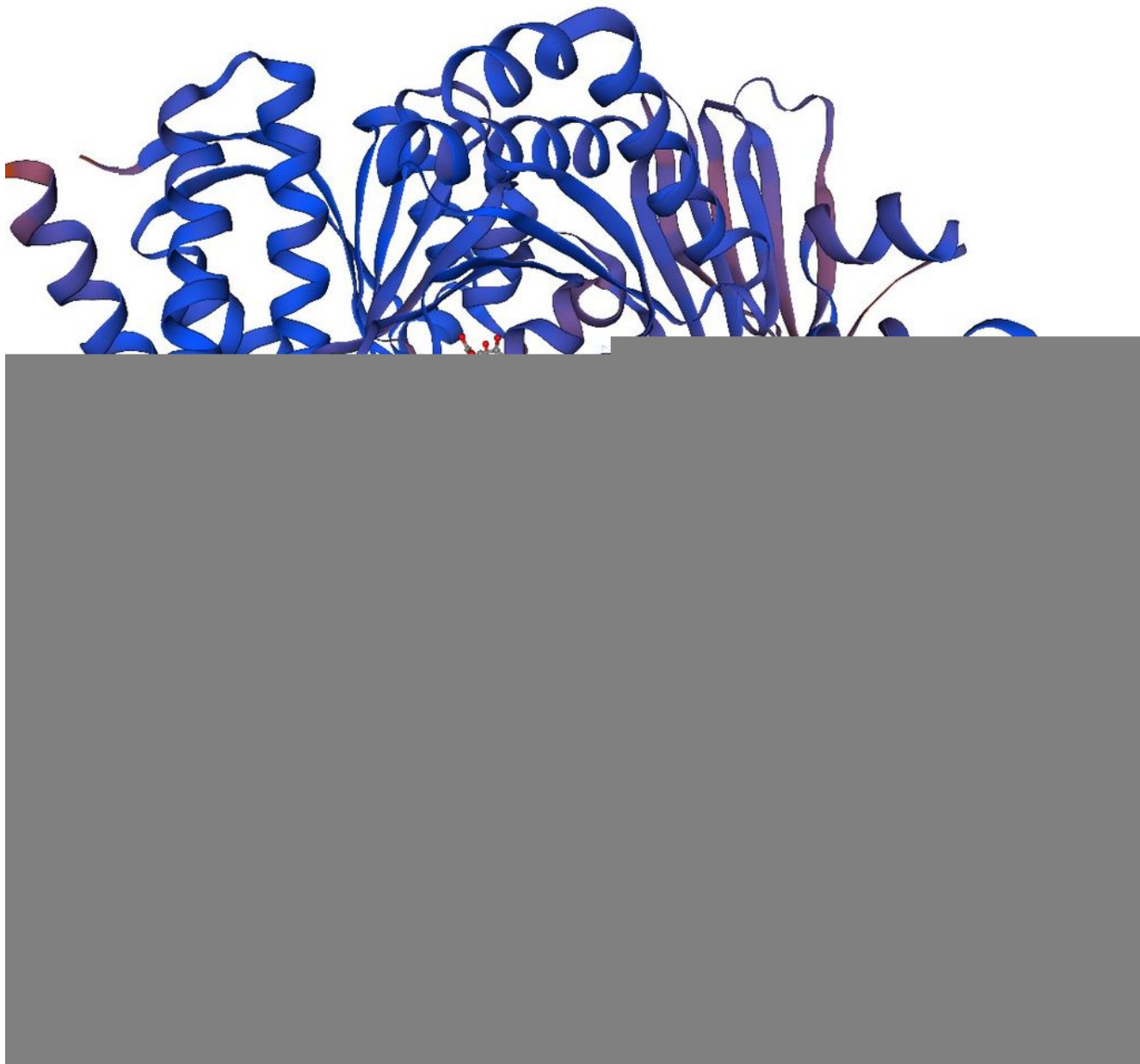

Figure 5

The predicted homology model of Richardson's ground squirrel NADP-IDH using the thirteen lined ground squirrel amino acid sequence as a reference (NCBI Reference Sequence: XP_005342105.1) .Model was generated using SWISS-MODEL.